Eur Biophys J (2012) 41:607–614
DOI 10.1007/s00249-012-0828-2

ORIGINAL PAPER

EBSA
Biophysics in Europe

Probing the catalytic allosteric mechanism of rabbit muscle pyruvate kinase by tryptophan fluorescence quenching

Feng Li · Ting Yu · Yuwei Zhao · Shaoning Yu

Received: 23 March 2012 / Accepted: 28 May 2012 / Published online: 12 July 2012

Abstract Pyruvate kinase acts as an allosteric enzyme, playing a crucial role in the catalysis of the final step of the glycolytic pathway. In this study, site-specific mutagenesis and tryptophan fluorescence quenching were used to probe the catalytic allosteric mechanism of rabbit muscle pyruvate kinase. Movement of the B domain was found to be essential for the catalytic reaction. Rotation of the B domain in the opening of the cleft between domains B and A induced by the binding of activating cations allows substrates to bind, whereas substrate binding shifts the rotation of the B domain in the closure of the cleft. Trp-157 accounts for the differences in tryptophan fluorescence signal with and without activating cations and substrates. Trp-481 and Trp-514 are brought into an aqueous environment after phenylalanine binding.

Keywords Pyruvate kinase · Fluorescence · Quenching · Conformational change · Allosteric mechanism · Catalysis · Glycolytic pathway

Abbreviations

PK	Pyruvate kinase
CD	Circular dichroism
FT-IR	Fourier transform infrared spectroscopy
ADP	Adenosine diphosphate
PEP	Phosphoenolpyruvate
TMK buffer	50 mM Tris, 8 mM $MgSO_4$, and 75 mM KCl at pH 7.5
Phe	Phenylalanine
GdnHCl	Guanidine hydrochloride

Feng Li and Ting Yu equally contribute to this work.

F. Li · T. Yu · Y. Zhao · S. Yu (✉)
Department of Chemistry, Fudan University,
Shanghai 200433, China
e-mail: yushaoning@fudan.edu.cn

Introduction

As a regulatory glycolytic enzyme, rabbit muscle pyruvate kinase (PK) requires activating cations and substrates to catalyze the conversion of phosphoenolpyruvate (PEP) to pyruvate (Boyer et al. 1942; Gupta et al. 1976; Mattevi et al. 1996). Structurally, PK is a homo-tetramer composed of four chemically identical subunits with approximately 530 residues in each monomer. The four subunits form two interfaces that are approximately perpendicular; namely, the Y-interface comprising the C- and N-terminal domains of monomer pairs 1–2 and 3–4, and the Z-interface comprising all four domains between monomer pairs 1–3 and 2–4 (Fig. 1; Larsen et al. 1994; Muirhead et al. 1986). The PK monomer contains four principal domains: N-terminal domain (residues 1–42), domain A (residues 43–115 and 219–387), domain B (residues 116–218), and domain C (residues 388–530; Larsen et al. 1997; Muirhead et al. 1986). On the basis of structural information, domain B protrudes into the solvent and forms a cleft with domain A (Larsen et al. 1994). These two domains are connected by a flexible hinge region. The active site is located in the pocket between domains A and B of the same subunit (Consler and Lee 1988; Muirhead et al. 1986).

A variety of techniques have been used to explore changes in the conformation of pyruvate kinase in response to ligand binding (Carminat et al. 1971; Kayne and Price 1972; Kayne and Suelter 1965; Mildvan and Cohn 1965, 1966; Oria-Hernandez et al. 2005; Ou et al. 2010; Suelter 1967; Suelter et al. 1966; Yu et al. 2003). Kinetic data

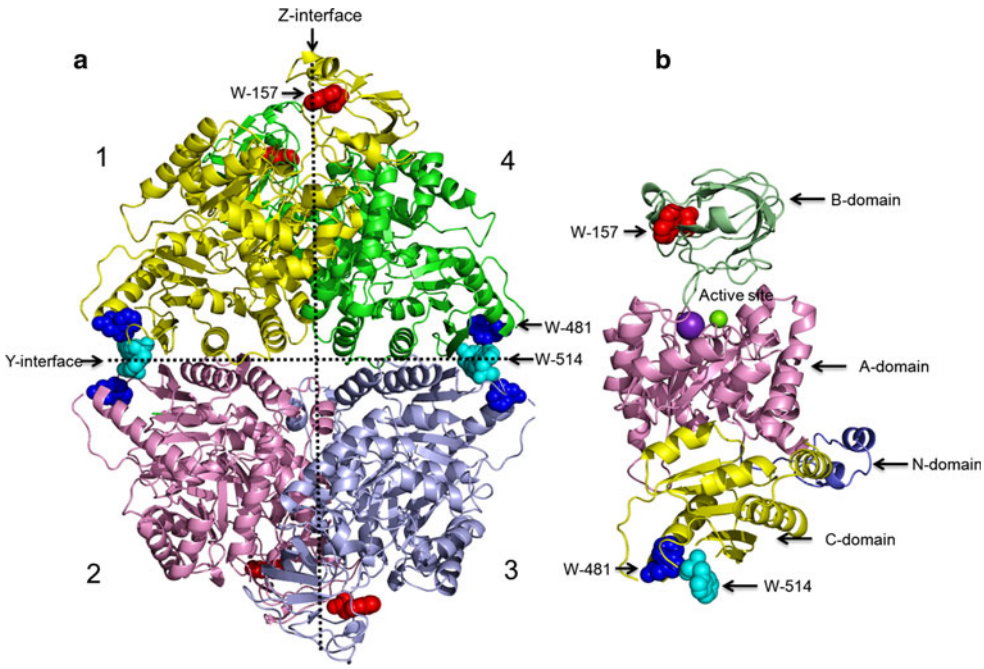

Fig. 1 **a** Structure of rabbit muscle PK homo-tetramer: monomer 1 (*yellow*), monomer 2 (*pink*), monomer 3 (*light blue*), monomer 4 (*green*). The Y-interface and Z-interface are marked with a *dashed line*. Tryptophan residues: Trp-157 (*red*), Trp-481 (*blue*), and Trp-514 (*cyan*). **b** Structure of the rabbit muscle PK monomer. Each monomer consists of the N-terminal domain (*slate*), domain A (*pink*), domain B (*pale green*), and domain C (*yellow*). There are three tryptophan residues: Trp-157 (*red*), Trp-481 (*blue*), and Trp-514 (*cyan*). Metal cations: K (*violet*), Mg (*green*). The active site is situated between the A and B domains

indicate that K^+ is directly involved in the acquisition of the active conformation and movement of the B domain of PK (Oria-Hernandez et al. 2005). The results of structural dynamics indicate that PK exhibits a more dynamic structure after binding activating metal ions and substrates, whereas binding Phe decreases the dynamics (Yu et al. 2003).

Ultraviolet and fluorescence spectra of PK have revealed that one or more tryptophan residues were transferred from the non-aqueous to aqueous environment during the conformational transition. Changes in the tryptophan residues of the solvating environment could indirectly reflect the protein's conformational changes (Kayne and Suelter 1965; Suelter 1967). Three tryptophan residues are present per PK monomer: Trp-157 is in domain B and close to the active site, whereas Trp-481 and Trp-514 are in domain C and close to the Y-interface (Larsen et al. 1997; Muirhead et al. 1986). These tryptophan residues can be used as indicators of the conformational changes induced by ligand binding. The previous fluorescence acrylamide quenching analysis has indicated that interactions with Mg^{2+} and K^+ lead to more exposed tryptophan residues of PK while interactions with PEP and ADP decreased solvent accessibility of the tryptophan residues (Ou et al. 2010). However, the results cannot confirm the contribution of every tryptophan residue on the fluorescence signal changes of PK induced by ligand binding.

In this work, tryptophan fluorescence quenching was used to probe the catalytic allosteric mechanism of PK. To avoid signal interference among different tryptophan's, two mutants, namely W481A/W514A-PK and W157A-PK, were designed to address these issues.

Materials and methods

Materials

Disodium salt of ADP, tricyclohexylammonium salt of PEP, phenylalanine, NADH, and LDH type II were purchased from Sigma. Tris and acrylamide were obtained from Amresco. KCl and $MgSO_4$ were purchased from Sinopharm Chemical Reagent Co., Ltd.

Site-directed mutagenesis

Plasmid pET22b containing the wild-type PK gene was kindly provided by Dr. George H. Reed from the University of Wisconsin (Madison, WI). Mutants for W157A-PK and W481A/W514A-PK were constructed using the Quik Change Site-Directed Mutagenesis Kit according to the manufacturer's protocol (Stratagene) with plasmid pET22b encoding WT-PK as a template. The mutant for W157A-PK was created by replacing W157 with alanine using the following primer pair: W157A, sense 5′-GCGACGAGAACATCCTGGCGCTGGACTACAAGAACATTTGCAAG-3′, antisense 5′-TGTTCTTGTAGTCCAGCGCCAGGATGTTCTCGTCGCACTTCT-3′. The double mutant for W481A/W514A-PK was created by replacing W481 and W514 with alanine using the following primer pairs: W481A, sense 5′-CGC-TGGAGGCCGTCCGCATGCAGCACCTGATAGCTC-3′, antisense 5′-GGAGGTC-GACATCCTCAGCCGCGGCCTCCTGGACCGGATCCTT-3′; W514A, sense 5′-G-GATCCGGTCCAGGAGGCCGCGGCTGAGGATGTCGACCTCCGG-3′, antisense 5′-GAAGCCAGAGCCAGGGCGCGCTCCGGTGAGCACAA

TGACCACAT-3′. The sequences of the PK mutants were verified by DNA sequencing.

Protein purification and preparation

Wild-type PK and two PK mutants were purified from IPTG-induced *Escherichia coli* strain BL21 according to published procedures (Laughlin and Reed 1997). The protein purity was assessed by staining SDS–PAGE gels with Coomassie Blue. Glycerol (20 %) was added to the purified protein solution, which was stored at −20 °C. The PK solution was dialyzed against 50 mM Tris buffer (pH 7.5) overnight to remove glycerol and other additives with three buffer changes before being used. The concentration of PK solution was determined spectrophotometrically by using the extinction coefficient of 0.54 ml/(mg cm) at 280 nm (Oberfelder et al. 1984). High concentrated PK was obtained by centrifugation using an Amicon Ultra-4 (Millipore Corporation, Billerica, USA).

Pyruvate kinase activity assays

A coupled assay procedure with lactate dehydrogenase in TMK buffer containing 0.3 mM NADH and 0.05 mg/ml LDH was used to determine the enzymatic activity of PK (Bucher and Pfleiderer 1955). The concentration for both of ADP and PEP in the mixture was 2 mM. Finally, the reaction was initiated by the addition of 10 µl of 0.06 mg/ml PK.

Secondary structure determination

The secondary structure of PK was monitored by CD and FT-IR spectroscopy. The CD spectra were routinely recorded with a JASCO-810 spectropolarimeter (Jasco, Japan) from 360 to 195 nm (far-UV, 195–250 nm and near-UV, 250–360 nm) using a slit program yielding a 1.5-nm bandwidth per wavelength. 0.05 and 1.0 cm fused silica cells were used for far-UV and near-UV spectra, respectively. Six repetitive scans were obtained and averaged for each experimental condition at room temperature (25 ± 3 °C). The concentration of the protein solution was 0.25 mg/ml in each experiment.

FT-IR spectra were recorded with an ABB Bomem (Quebec, Canada) MB-3000 Fourier Transform Infrared Spectrometer equipped with a dTGS detector and purged constantly with dry air. PK solutions of approximately 10 mg/ml were warmed to room temperature (25 ± 3 °C) and then loaded in a CaF_2 cell with a 7.5 µm spacer. The 200-scan single-beam spectra of protein samples, 50 mM Tris buffer (pH 7.5), and air were all collected with a 4 cm^{-1} resolution at a rate of three scans per second. The spectra for protein and buffer solutions were obtained by using a previously established protocol (de Rooij et al. 1998; Dong and Caughey 1994; Dong et al. 1990). In order to judge the success of water subtraction, a straight baseline between 2,000 and 1,750 cm^{-1} was used. Second-derivative spectra for the protein samples and buffer were obtained with a seven-point Savitsky–Golay derivative function, baseline corrected as described (Dong and Caughey 1994; Dong et al. 1990; Yu et al. 2004).

Fluorescence acrylamide quenching

Fluorescence intensity was measured by a Varian Cary Eclipse fluorescence spectrometer (Pal Alto, CA, USA) using a 1-cm quartz cuvette at room temperature (25 ± 3 °C). The excitation and emission wavelengths were 295 and 340 nm, respectively. The protein concentration was 0.25 mg/ml. The reaction mixtures were titrated with 4.0 M acrylamide in the reaction buffer (50 mM Tris buffer at pH 7.5). Four cuvettes (designated as A, B, C, and D) containing different solutions were used for the measurement. Cuvettes A, B, and C contained 0.25 mg/ml protein in buffer, and cuvette D contained buffer only. During the experiment, no buffer or acrylamide was titrated into cuvette A, and the readings were used to validate instrument stability. Cuvettes B and C were titrated with the same volume of buffer and acrylamide, respectively. Aliquots of acrylamide were titrated into cuvette *D*. As a consequence of all effects on the observed fluorescence intensity, the actual fluorescence intensity fraction can be described as:

$$F = (F_C/F_B) - F_D \quad (1)$$

where F_B, F_C, and F_D are the observed signal fractions of protein fluorescence in cuvettes *B*, *C*, and *D*, respectively. For every point, the fluorescence intensity was read at least three times to ensure accuracy. Quenching data were plotted using the Stern–Volmer equation (Chen and Lee 2003):

$$F_0/F = (1 + K_{SV}(Q))(1 + V(Q)) \quad (2)$$

where F_0/F is the fractional decrease in fluorescence due to the quencher (Q), and K_{SV} and V are the collisional and static quenching constants, respectively.

Results

Enzymatic assay

The enzymatic activity of WT-PK and the two mutants was monitored by the decrease in absorbance at 340 nm for 500 s. The reaction rate was measured from the initial linear region of the curve. The results indicated that the

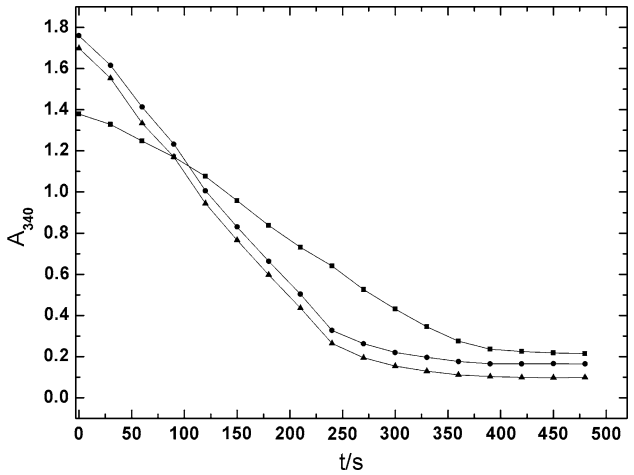

Fig. 2 The enzymatic activity of WT-PK (*filled circle*), W481A/W514A-PK (*filled triangle*), and W157A-PK (*filled square*)

activity of W481A/W514A was very close to that of WT, whereas W157A was less active than WT (Fig. 2).

Secondary structure

CD and FT-IR spectroscopes were used to determine the secondary structure of PK. The results are shown in Fig. 3. The CD spectra show that the WT and the two mutants exhibited typical CD curves and were essentially identical in both the near-UV and far-UV region (Fig. 3a). The second-derivative FT-IR spectra of the amide I band for WT and the two mutants are shown in Fig. 3b. The results indicate that mutation of the tryptophan residues did not elicit any observable difference in the secondary structure of PK.

Interaction with activating cations

The accessibility of the tryptophan residues of WT-PK and the two mutants induced by the binding of activation cations was quantitatively assessed using acrylamide collisional quenching. The tryptophan residues of WT-PK (Fig. 4a) and W481A/W514A-PK (Fig. 4b) in TMK buffer were more accessible than residues in 50 mM Tris buffer (pH 7.5), but similar to 8 mM Mg^{2+}. The tryptophan residues of WT-PK and W481A/W514A-PK in 75 mM K^+ were more exposed than residues in 50 mM Tris buffer (pH 7.5), but less exposed in TMK buffer. In regard to W157A-PK (Fig. 4c), the binding of activating metal ions did not lead to visible changes in the results. These results indicate that Mg^{2+}, as well as K^+ or the combination of K^+ and Mg^{2+}, increase the solvent exposure of Trp-157. Compared to the previous study, these results clearly indicate that the majority of changes in tryptophan fluorescence signal from PK induced by the binding of activating cations come from

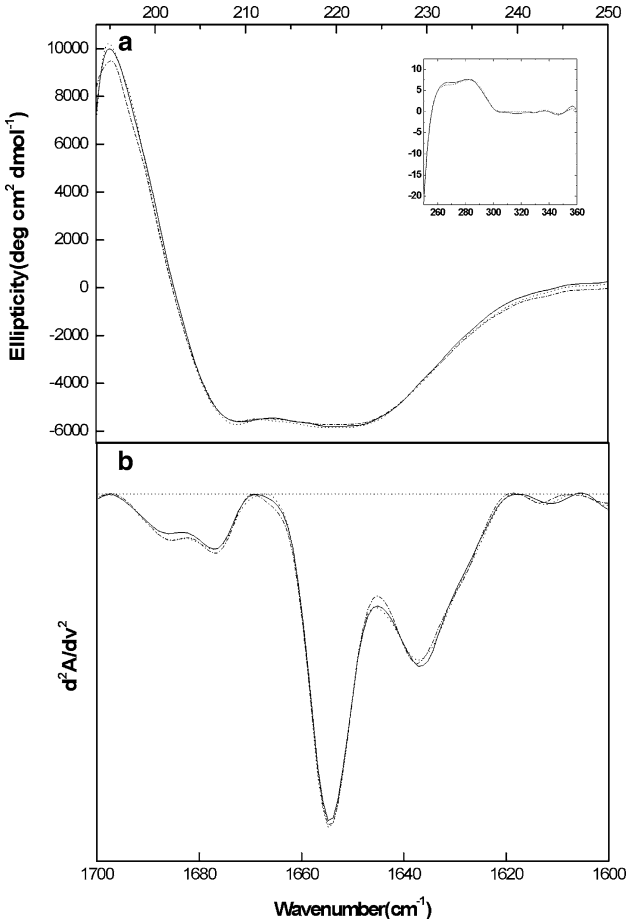

Fig. 3 **a** CD spectra of 0.25 mg/ml PK in TMK buffer at 23 °C. The insert is the near-UV CD spectra. The *lines* are: CD spectra of WT-PK (*solid line*), W481A/W514A-PK (*dashed line*), and W157A-PK (*dashed dot line*). **b** The second-derivative amide I spectra of WT-PK (*solid line*), W481A/W514A-PK (*dashed line*), and W157A-PK (*dashed dot line*)

Trp-157 (Kayne and Suelter 1965; Ou et al. 2010; Suelter 1967).

Interaction with substrates

After substrate binding, the tryptophan residues of WT-PK (Fig. 5a) were less accessible in the presence of 2 mM PEP-TMK buffer or ADP-PEP-TMK buffer than residues in 50 mM Tris buffer (pH 7.5), and much less than residues in TMK buffer. The accessibility of the tryptophan residues of WT-PK in 2 mM ADP-TMK buffer was close to the accessibility observed in TMK buffer, indicating that ADP contributes little to the solvent accessibility of tryptophan residues, which is consistent with earlier observations (Suelter et al. 1966). The experiment with W481A/W514A-PK (Fig. 5b) yielded parallel results to WT-PK. For W157A-PK (Fig. 5c), interaction with substrates clearly did not induce significant changes in the accessibility of tryptophan residues,

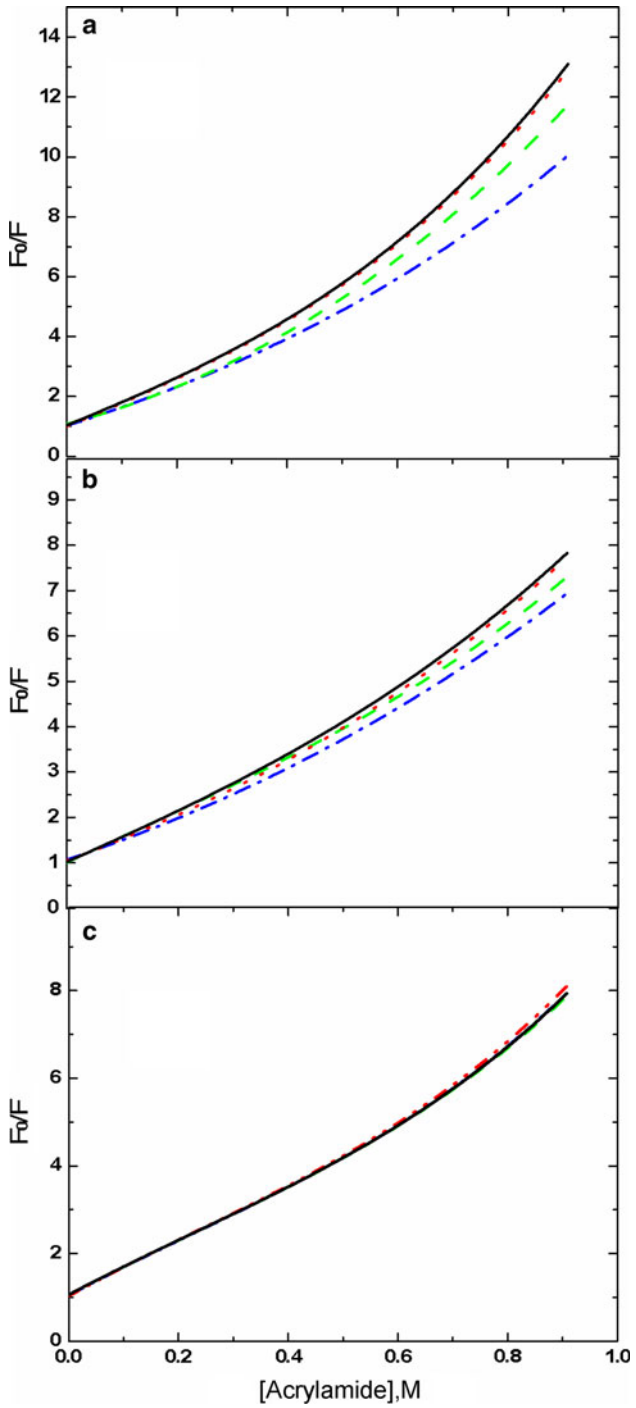

Fig. 4 Acrylamide quenching of the tryptophan fluorescence of 0.25 mg/ml PK in buffer at 23 °C. **a** WT-PK; **b** W481A/W514A-PK; **c** W157A-PK. The solution compositions are: 50 mM Tris buffer at pH 7.5 (*blue dash dot line*); 75 mM KCl, 50 mM Tris buffer at pH 7.5 (*green dash line*); 8 mM $MgSO_4$, 50 mM Tris buffer at pH 7.5 (*red dot line*); TMK buffer (*black solid line*). The *solid curves* are the best-fit lines

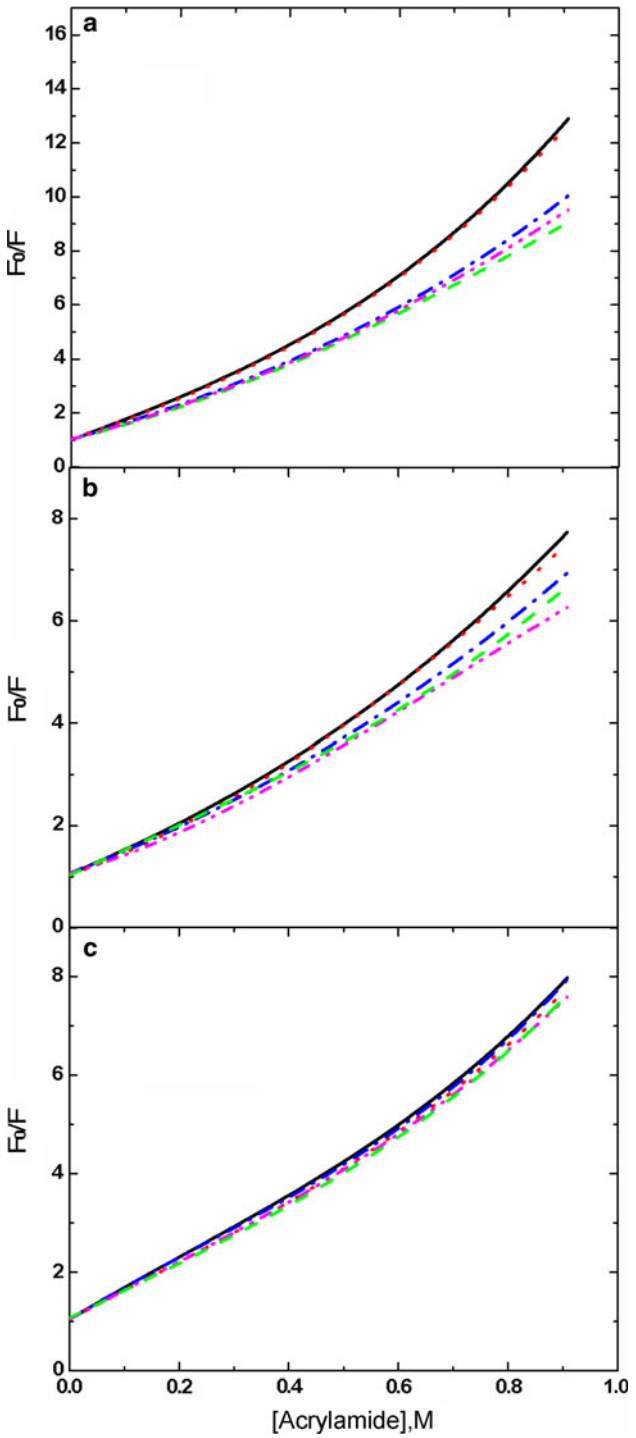

Fig. 5 Acrylamide quenching of the tryptophan fluorescence of 0.25 mg/ml PK at 23 °C. **a** WT-PK; **b** W481A/W514A-PK; **c** W157A-PK. The solution compositions are: 50 mM Tris buffer at pH 7.5 (*blue dash dot line*); TMK buffer (*black solid line*); 2 mM ADP, TMK buffer (*red dot line*); 2 mM PEP, TMK buffer (*magenta dash dot line*); 2 mM ADP, 2 mM PEP, TMK buffer (*green dash line*). The *solid curves* are the best-fit lines

suggesting that the binding of PEP or ADP/PEP has no influence on the accessibility of Trp-481 and Trp-514. Thus, the interaction with PEP decreased the solvent exposure of Trp-157 and the majority of changes in the tryptophan fluorescence signal from PK induced by the binding of substrates come from Trp-157.

Interaction with inhibitor and denaturant

The results of inhibitor (Phe) and denaturant (GdnHCl) interaction reveal that the accessibility of the tryptophan residues of WT-PK (Fig. 6a) and W157A-PK (Fig. 6c) in 12 mM Phe-TMK buffer was close to that of residues in 0.5 M GdnHCl-50 mM Tris buffer (pH 7.5), and exceeded that of TMK buffer. The tryptophans in W481A/W514A-PK (Fig. 6b) were more accessible in the 12 mM Phe-TMK buffer than in the 50 mM Tris buffer (pH 7.5), and less accessible than in the presence of 0.5 M GdnHCl-50 mM Tris buffer (pH 7.5). The result for W481A/W514A-PK in the presence of 12 mM Phe-TMK buffer was similar to the result obtained in TMK buffer, suggesting that the binding of Phe has very little effect on the solvent exposure of Trp-157. These results suggest that Trp-481 and Trp-514 are more open to solvent with the binding of Phe.

Discussion

PK serves as an allosteric enzyme, playing a crucial role in catalyzing the final step of the glycolytic pathway (Mattevi et al. 1996). Full enzymatic activity requires binding of two equivalents of divalent cation and an activating monovalent cation such as K^+ (Boyer et al. 1942; Gupta et al. 1976). As an essential activator of PK, evidence that K^+ was involved in the movement of the B domain and acquisition of active conformation of PK was reported (Oria-Hernandez et al. 2005). The X-ray analysis of the rabbit M1 protein in complex with pyruvate has identified the residues forming the PEP and cation binding sites, which are located in the cleft between the A and B domains, and are mostly provided by the sixth and eighth loops of the A domain (Larsen et al. 1994). The fact that conformational changes are correlated to changes in enzymatic activity allows one to envision an alteration in structure at the active site as being responsible for the functional change. Thus, it is conceivable that the movement of domain B relative to domain A may open or close the active site cleft in response to substrates or effectors (Consler et al. 1988).

The FT-IR and CD experiments reveal that no change was observed in the secondary structure of WT-PK and the two mutants. In the enzymatic assay, the activity of W157A-PK was weaker than that of wild-type and the double mutant (Fig. 2). However, the fluorescence intensity of W157A-PK would not be affected because the two tryptophan residues, Trp-481 and Trp-514, are located in the C domain far from the active site.

The accessibility of the tryptophan residues of PK induced by ligand binding was quantitatively assessed using

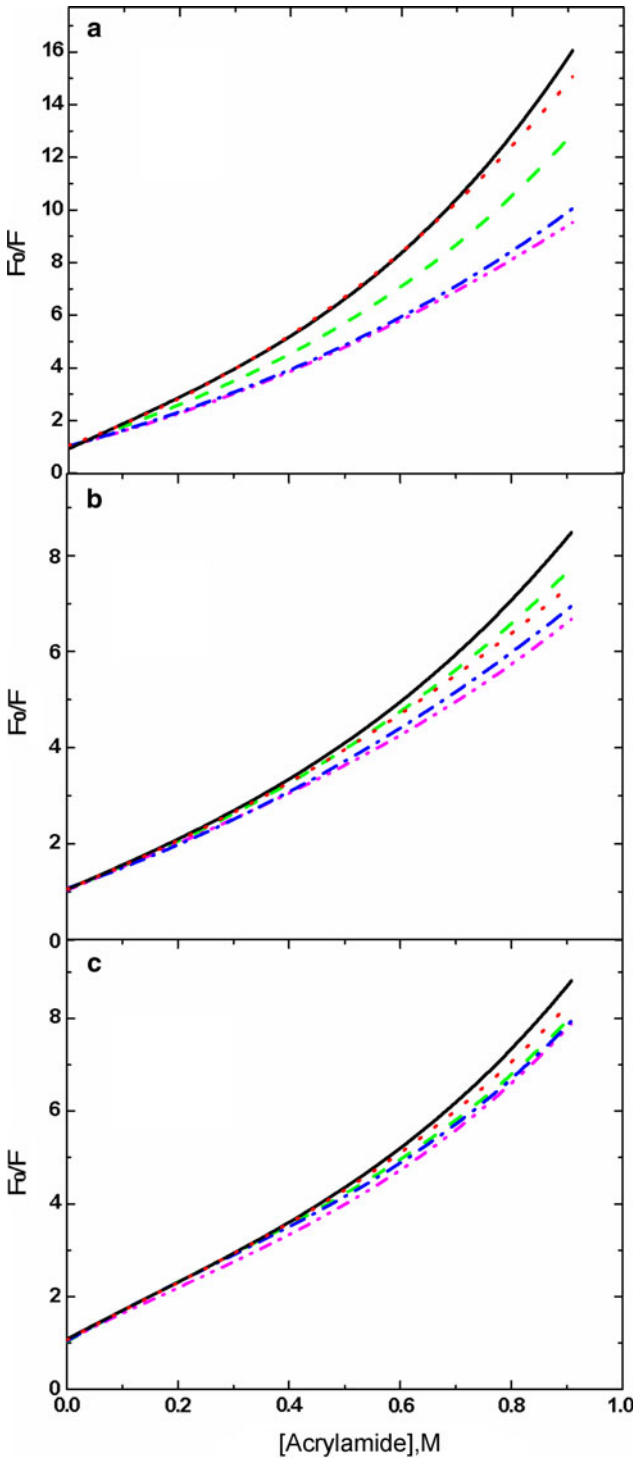

Fig. 6 Acrylamide quenching of the tryptophan fluorescence of 0.25 mg/ml PK at 23 °C. **a** WT-PK; **b** W481A/W514A-PK; **c** W157A-PK. The solution compositions are: 50 mM Tris buffer at pH 7.5 (*blue dash dot line*); TMK buffer (*green dash line*); 2 mM PEP, TMK buffer (*magenta dash dot line*); 12 mM Phe, TMK buffer (*red dot line*); 0.5 M GdnHCl, 50 mM Tris buffer at pH 7.5 (*black solid line*). The *solid curves* are the best-fit lines

acrylamide fluorescence collisional quenching (Figs. 4, 5, 6). The results clearly indicate that the binding of activating cations increased the exposure of Trp-157. In contrast, the interaction with PEP/K^+/Mg^{2+} or ADP/PEP/K^+/Mg^{2+} decreased the solvent accessibility of Trp-157. The solvent exposure of Trp-481 and Trp-514 induced by activating cations and substrates was not visible, which is consistent with the fact that the binding sites of activating cations and substrates of PK are close to the active site, which is far away from Trp-481 and Trp-514 (Stuart et al. 1979). Trp-157 is located in the B domain and very close to the active site. The solvent exposure of Trp-157 correlates with the solvent environment of the active site. In other words, the binding of activating cations results in the enzyme adopting an "open" conformation, whereas interaction with substrates results in a "closed" conformation. The C domain remains in the same position in the "open" and "closed" conformations, whereas the B domain is highly mobile and differs by 40° in the two conformers (Larsen et al. 1998). Thus, we can reasonably speculate that the exposure of the active site results from the movement of the B domain. The binding of activating cations causes rotation of the B domain in the opening of the cleft between the B and A domains, which allows substrates to bind. Substrate binding shifts the rotation of the B domain into the closure of the cleft. Moreover, the allosteric regulation of PK enables the catalytic reaction of ADP, PEP, and a proton to create ATP and pyruvate. The speculation is supported by the results that Trp157 accounts for differences in the tryptophan fluorescence signal in the presence and absence of activating cations and substrates.

The PK system can also be allosterically regulated by Phe (Carminat et al. 1971). The binding of Phe apparently perturbs the PK structure, as indicated by enhanced intrinsic protein fluorescence intensity (Kayne and Price 1972) and an altered UV spectrum (Kayne and Price 1972; Kwan and Davis 1980). Phe binds in a deep pocket between the A and C domains, far from the active site (Williams et al. 2006). Therefore, the binding of Phe may have little effect on the exposure of Trp-157. Fluorescence collisional quenching analysis of WT-PK and W157A-PK revealed that, in the presence of Phe/K^+/Mg^{2+}, tryptophan accessibility is close to the accessibility in 0.5 M GdnHCl-50 mM Tris buffer (pH 7.5) and exceeded the accessibility in K^+/Mg^{2+}, which is in contrast to that of PEP binding. However, the results for W481A/W514A-PK in the presence of Phe/K^+/Mg^{2+} parallel the results obtained in K^+/Mg^{2+}. These results support the hypothesis that Phe binding has little effect on the exposure of Trp-157 and reveal that Trp-481 and Trp-514 were brought into an aqueous environment after Phe binding. In other words, the binding of Phe shifts the Y-interface of PK to a more loose structure.

Conclusion

The movement of the B domain enables the catalytic reaction of ADP, PEP, and a proton to create ATP and pyruvate. Rotation of the B domain in the opening of the cleft between the B and A domains induced by the binding of activating cations allows either PEP or ADP to bind, whereas the binding of substrates shifts the rotation of the B domain to the closure of the cleft. Trp-157 accounts for the differences in the tryptophan fluorescence signal in the presence and absence of activating cations and substrates. Trp-481 and Trp-514 are brought into an aqueous environment after Phe binding.

Acknowledgments This project was supported in part by grants from the National Natural Science Foundation of China (No. 30970631), and Shanghai Leading Academic Discipline Project (No. B109).

References

Boyer PD, Lardy HA, Phillips PH (1942) The role of potassium in muscle phosphorylation. J Biol Chem 146:673–682

Bucher T, Pfleiderer G (1955) Pyruvate kinase from muscle: pyruvate phosphokinase, pyruvic phosphoferase, phosphopyruvate transphosphorylase, phosphate—transferring enzyme II, etc. Phosphoenolpyruvate + ADP ⇌ Pyruvate + ATP. Method Enzymol 1:435–440

Carminat H, Deasua LJ, Leiderma B, Rozengur E (1971) Allosteric properties of skeletal muscle pyruvate kinase. J Biol Chem 246:7284–7288

Chen R, Lee JC (2003) Functional roles of loops 3 and 4 in the cyclic nucleotide binding domain of cyclic AMP receptor protein from *Escherichia coli*. J Biol Chem 278:13235–13243

Consler TG, Lee JC (1988) Domain interaction in rabbit muscle pyruvate kinase. I. Effects of ligands on protein denaturation induced by guanidine hydrochloride. J Biol Chem 263:2787–2793

Consler TG, Uberbacher EC, Bunick GJ, Liebman MN, Lee JC (1988) Domain interaction in rabbit muscle pyruvate kinase. II. Small angle neutron scattering and computer simulation. J Biol Chem 263:2794–2801

de Rooij J, Zwartkruis FJT, Verheijen MHG, Cool RH, Nijman SMB, Wittinghofer A, Bos JL (1998) Epac is a Rap1 guanine-nucleotide-exchange factor directly activated by cyclic AMP. Nature 396:474–477

Dong A, Caughey WS (1994) Infrared methods for study of hemoglobin reactions and structures. Methods Enzymol 232:139–175

Dong A, Huang P, Caughey WS (1990) Protein secondary structures in water from second-derivative amide I infrared spectra. Biochemistry 29:3303–3308

Gupta RK, Oesterling RM, Mildvan AS (1976) Dual divalent cation requirement for activation of pyruvate kinase: essential roles of both enzyme- and nucleotide-bound metal ions. Biochemistry 15:2881–2887

Kayne FJ, Price NC (1972) Conformational changes in the allosteric inhibition of muscle pyruvate kinase by phenylalanine. Biochemistry 11:4415–4420

Kayne FJ, Suelter CH (1965) Effects of temperature, substrate, and activating cations on the conformations of pyruvate kinase in aqueous solutions. J Am Chem Soc 87:897–900

Kwan C-Y, Davis RC (1980) pH-dependent amino acid induced conformational changes of rabbit muscle pyruvate kinase. Can J Biochem 58:188–193

Larsen TM, Laughlin LT, Holden HM, Rayment I, Reed GH (1994) Structure of rabbit muscle pyruvate kinase complexed with Mn^{2+}, K^+, and pyruvate. Biochemistry 33:6301–6309

Larsen TM, Benning MM, Wesenberg GE, Rayment I, Reed GH (1997) Ligand-induced domain movement in pyruvate kinase: structure of the enzyme from rabbit muscle with Mg^{2+}, K^+, and L-phospholactate at 2.7 Å resolution. Arch Biochem Biophys 345:199–206

Larsen TM, Benning MM, Rayment I, Reed GH (1998) Structure of the Bis(Mg^{2+})-ATP-oxalate complex of the rabbit muscle pyruvate kinase at 2.1 Å resolution: ATP binding over a barrel. Biochemistry 37:6247–6255

Laughlin LT, Reed GH (1997) The monovalent cation requirement of rabbit muscle pyruvate kinase is eliminated by substitution of lysine for glutamate 117. Arch Biochem Biophys 348:262–267

Mattevi A, Bolognesi M, Valentini G (1996) The allosteric regulation of pyruvate kinase. FEBS Lett 389:15–19

Mildvan AS, Cohn M (1965) Kinetic and magnetic resonance studies of the pyruvate kinase reaction. I. Divalent metal complexes of pyruvate kinase. J Biol Chem 240:238–246

Mildvan AS, Cohn M (1966) Kinetic and magnetic resonance studies of the pyruvate kinase reaction. II. Complexes of enzyme, metal, and substrates. J Biol Chem 241:1178–1193

Muirhead H, Clayden DA, Barford D, Lorimer CG, Fothergill-Gilmore LA, Schiltz E, Schmitt W (1986) The structure of cat muscle pyruvate kinase. EMBO J 5:475–481

Oberfelder RW, Lee LL, Lee JC (1984) Thermodynamic linkages in rabbit muscle pyruvate kinase: kinetic, equilibrium, and structural studies. Biochemistry 23:3813–3821

Oria-Hernandez J, Cabrera N, Perez-Montfort R, Ramirez-Silva L (2005) Pyruvate kinase revisited: the activating effect of K^+. J Biol Chem 280:37924–37929

Ou Y, Tao W, Zhang Y, Wu G, Yu S (2010) The conformational change of rabbit muscle pyruvate kinase induced by activating cations and its substrates. Int J Biol Macromol 47:228–232

Stuart DI, Levine M, Muirhead H, Stammers DK (1979) Crystal structure of cat muscle pyruvate kinase at a resolution of 2.6 Å. J Mol Biol 134:109–142

Suelter CH (1967) Effects of temperature and activating cations on the fluorescence of pyruvate kinase. Biochemistry 6:418–423

Suelter CH, Singleton R, Kayne FJ, Arrington S, Glass J, Mildvan AS (1966) Studies on the interaction of substrate and monovalent and divalent cations with pyruvate kinase. Biochemistry 5:131–139

Williams R, Holyoak T, McDonald G, Gui C, Fenton AW (2006) Differentiating a ligand's chemical requirements for allosteric interactions from those for protein binding. Phenylalanine inhibition of pyruvate kinase. Biochemistry 45:5421–5429

Yu S, Lee LLY, Lee JC (2003) Effects of metabolites on the structural dynamics of rabbit muscle pyruvate kinase. Biophys Chem 103:1–11

Yu SN, Mei FC, Lee JC, Cheng XD (2004) Probing cAMP-dependent protein kinase holoenzyme complexes I alpha and II beta by FT-IR and chemical protein footprinting. Biochemistry 43:1908–1920